ELSEVIER

Journal of Nuclear Materials 258–263 (1998) 1097–1103

journal of nuclear materials

Material damage and thermal response of LHD divertor mock-ups by high heat flux

K. Tokunaga [a,*], N. Yoshida [a], Y. Kubota [b], N. Noda [b], O. Motojima [b], D.L. Youchison [c], R.D. Watson [c], R.E. Nygren [c], J.M. McDonald [c], T.D. Marshall [c]

[a] *Research Institute for Applied Mechanics, Kyushu University, Kasuga, Fukuoka 816, Japan*
[b] *National Institute for Fusion Science, Toki, Gifu 509-52, Japan*
[c] *Sandia National Laboratories, Albuquerque, NM 87185, USA*

Abstract

Mockups for tests were fabricated and thermal response and thermal fatigue lifetime tests using electron beam facilities were carried out to examine material damage and thermal response of carbon carbon fiber composite (CFC) brazed the oxygen free high conductivity (OFHC) for a local island divertor (LID) plate. Model calculation for thermal response was also carried out to explain the phenomena of experimental results. Thermal response tests of an MFC-1 mockup were performed at the condition that the water flow velocity, pressure and temperature were 1.6–10 m/s, 1.0–4.0 MPa and 20°C, 150°C respectively. The MFC-1 mockup showed good heat removal performance. In the case of a CX-2002U mockup with 10 mm armor thickness, surface temperature is near 1000°C at 10 MW/m^2. Therefore, use of CX-2002U as armor material is allowable concerning the maximum surface temperature due to heat flux. A thermal fatigue test of the MFC-1 mockup was also performed. Temperatures increase due to degradation was not observed up to 1000 cycles. Calculation for thermal response was performed using a finite element analysis code. The comparison measured with calculated data presented information of critical heat flux and detachment of the tile.

1. Introduction

In the large helical device (LHD), which is under construction at the National Institute for Fusion Science, a local island divertor (LID) as well as a helical divertor is going to be used [1,2]. Mechanical joint type for the helical divertor will be used in the start up phase because maximum heat flux of the helical divertor is estimated to be 0.75 MW/m^2. On the other hand, the LID divertor plate of the LHD will be subjected to maximum heat flux of 10 MW/m^2 for steady state. Therefore, armor brazed on the oxygen free high conductivity copper (OFHC) is going to be used as the LID divertor plate [3,4]. To assess the material lifetime and thermal performance, investigation of the material damage and the thermal response due to high heat load is of importance [5,6]. In this study, test mockups were fabricated and thermal response and thermal fatigue lifetime tests using electron beam facilities were carried out to examine material damage and thermal response of carbon carbon fiber composite (CFC) brazed on the OFHC for the LID divertor plate. Model calculations for the thermal response were also carried out to explain the experimental results.

2. Experimental

2.1. Description of mockups

A schematic illustration of the mockup is shown in Fig. 1. The mockup is of a flat plate type. Three carbon blocks were brazed on the OFHC with the cooling tube. The dimensions of the carbon tiles are 23 mm × 30 mm

* Corresponding author. Tel.: +81 92 583 7986; fax: +81 92 582 7690; e-mail: tokunaga@riam.kyushu-u.ac.jp.

0022-3115/98/$19.00
PII: S0022-3115(98)00391-2

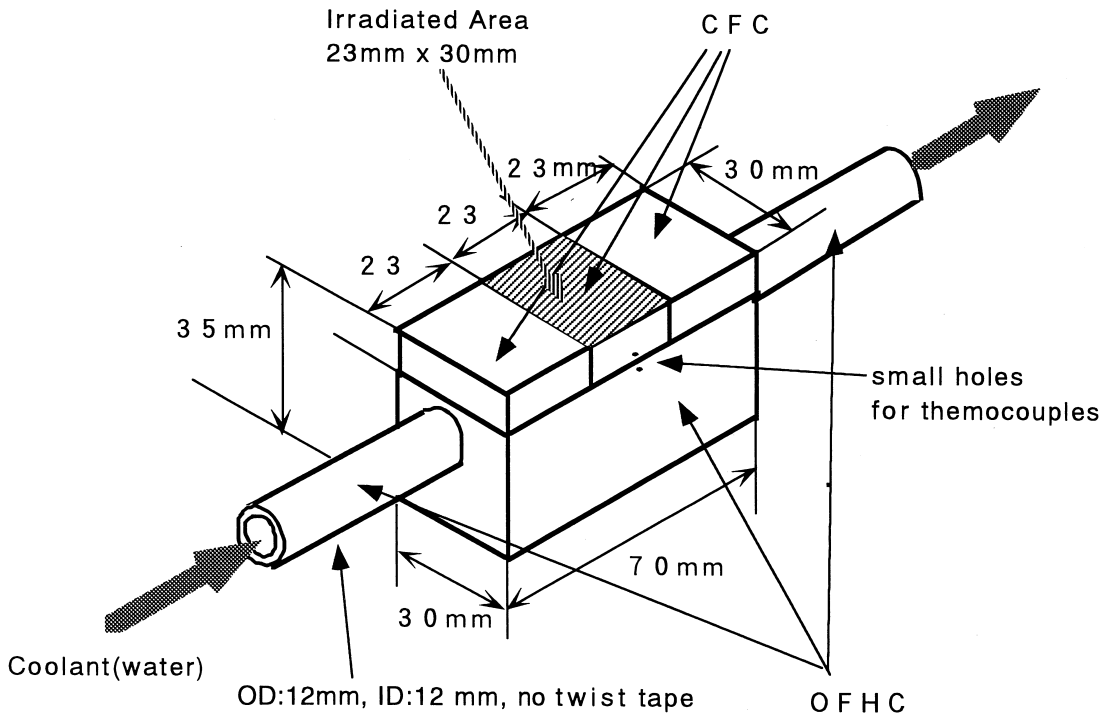

Fig. 1. Schematic illustration of test mockup.

on the surface at 10 mm thickness. Two types of carbon materials were used. These were 1D-CFC MFC-1 (Mitsubishi Chemical) [7] and 2D-CFC CX-2002U(Toyo Tanso) [8]. These carbon materials have a high thermal conductivity (MFC-1 :30/30/650 (W/mK), CX-2002U: 390/320/190 (W/mK)). The direction of the highest thermal conductivity of the CFCs was normal to the brazed area. Two holes for the thermocouple inserted were equipped with 1.5 mm DIA around the brazing (Fig. 1). Depth of the holes was 11 mm from the side face of the mockup. The carbon blocks are attached by brazing material (0.63Ag–0.3525Cu–0.0175Ti) at a temperature higher than 800°C by Mitsubishi Heavy Industries, Ltd.

2.2. Test procedures

Heat load tests for the mockups were performed with the use of electron beam test system (EBTS) [9] at Sandia National Laboratories (SNL) and actively cooling test stand (ACT) [10] at National Institute for Fusion Science (NIFS). In the EBTS, the thermal response tests for the MFC-1/OFHC were performed at the condition of cooling water as shown in Table 1. The conditions of (a)–(c) in Table 1 corresponded to that of test in ACT, most aggressive cooling and least aggressive (worst) cooling conditions, respectively. The electron beams were uniformly irradiated for 240 s on the surface of the center block (23 mm × 30 mm area). The surface temperature in the heated area was measured with optical pyrometers. The temperatures on both sides of the brazed area were measured with thermocouples which were inserted into the mockup. Heat flux was estimated using calorimetry which measure temperature difference between inlet and outlet. Tests for velocity change were also performed at the condition of the temperature and the pressure of inlet water and corresponded to (a)–(c) in Table 1.

Thermal fatigue and component lifetime of the MFC-1 mockup were investigated using the EBTS. Heat

Table 1
Conditions of temperature, pressure and velocity of cooling water in EBTS

Condition	Temperature (°C)	Pressure (MPa)	Standard velocity (m/s)	Velocity range (m/s)
(a)	20	1.0	7.5	1.6–10.0
(b)	20	4.0	10.0	2.4–10.0
(c)	150	1.5	5.0	1.6–8.4

flux, temperature, pressure and flow velocity of cooling water of the thermal fatigue test were 10 MW/m^2, 20°C, 1.0 MPa and 10 m/s, respectively. Irradiation time was 16–20 s and the number of cycles was 1000. After the heat load tests, surface modification and compositional changes were examined with a scanning electron microscope equipped with an energy dispersion X-ray spectroscope (SEM-EDS).

In the ACT, the thermal response tests for the CX-2002U/OFHC were examined at conditions of pressure of coolant water of 0.5 MPa, flow velocity of 8.0 m/s, inlet temperature of 20°C.

2.3. Modeling method for thermal response

Steady-state temperature profiles for a two dimensional cross-section of the mockups were calculated using the finite element analysis code ABAQUS [11]. Heat transfer from the mockup to the coolant water via forced convection was computed by ABAQUS using a user supplied film subroutine, which calculated the heat transfer coefficient as a function of wall temperature. The film subroutine version used here contains the Sieder–Tate correlation [12] for single heat transfer and the Thom correlation [13] for fully developed nucleate boiling heat transfer. For thermal conductivity, temperature dependence data has been used.

3. Results and discussion

3.1. Experimental results

Fig. 2 shows a plot of steady state temperatures of the surfaces, the upper and lower sides of interface of the brazed area of the MFC-1 mockup as a function of absorbed heat flux in the EBTS. The temperature, pressure and flow velocity were 20°C, 1.0 MPa and 7.5 m/s, respectively (condition (a) in Table 1). Results from the tests of the CX-2002U mockup in the ACT are overlaid. In the case of the ACT, the pressure of cooling water was 0.5 MPa. It is known that this pressure difference of the two cases does not influence the thermal response [14]. It can be seen from the figure that temperatures increase with increasing absorbed heat flux. The temperature rise of the surface of MFC-1 mockup was lower than that of the CX-2002U mockup. For example, at a heat flux of 10 MW/m^2, the surface temperature rise of the MFC-1 mockup was about 820°C but that of CX-2002U was about 1000°C. This

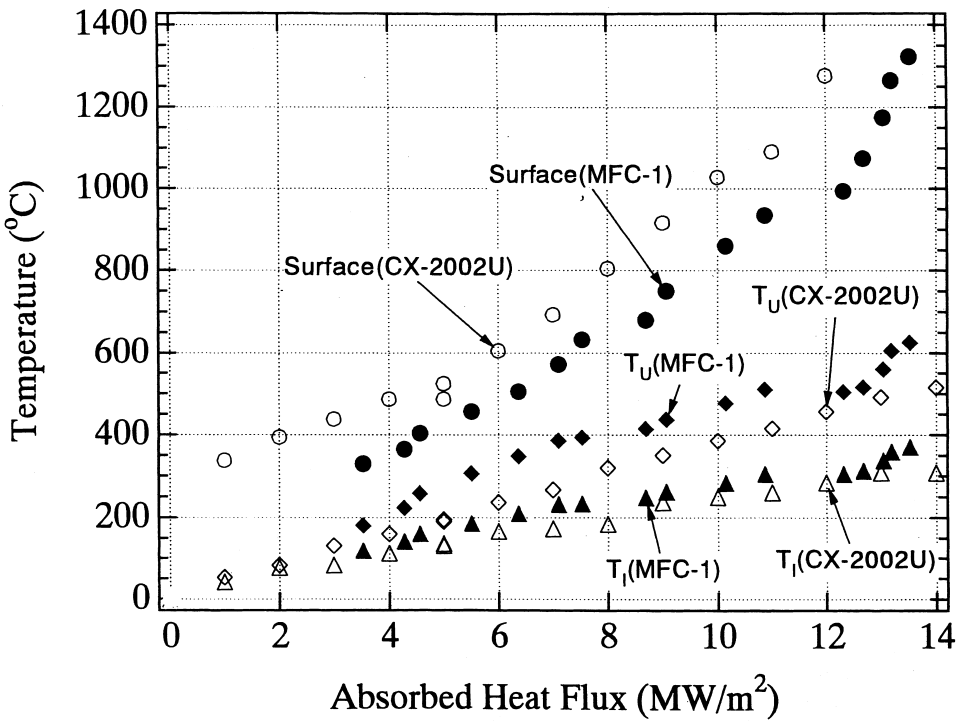

Fig. 2. Steady state temperature versus absorbed heat flux. Circle (surface), diamond (Tu) and triangle (T_l) show temperatures on surface, upper side and lower side of the brazed area. Black shading marks show the results of MFC-1 in EBTS mockup and unshaded marks show results of CX-2002U in ACT.

temperature difference is expected to be due to the difference in thermal conductivity of the two materials. Comparison with other data of heat flux tests in the ACT showed that temperature rise of the surface of MFC-1 is lowest [15]. This result indicated that the use of MFC-1 for armor materials realizes good heat removal performance. On the other hand, the temperature at the joint of the MFC-1 mockup was higher than that of the CX-2002U as shown in Fig. 3. This is assumed to be due to a lower temperature difference between the surface and the upper side of the brazing area by the higher thermal conductivity of the MFC-1. These results suggest that the temperature limit of the interface may be of importance.

Fig. 3 shows a plot of steady state temperatures of the MFC-1 mockup at most (b) and least aggressive cooling condition (c) shown in Table 1. For example, at 10 MW/m^2, surface temperatures are 700°C and 1100°C, respectively. It is expected that results of EBTS data would be between the results at these two conditions.

Fig. 4 shows surface temperatures as a function of the cooling water velocity at a heat flux of about 10 MW/m^2 at the condition that cooling water temperature and pressure were (a)–(c) in Table 1. It can be seen that temperature increases with decreasing velocity. These results show the temperature rise depends strongly on the water flow velocity.

Fig. 5 shows the change of temperature at the surface, the upper side (T_u) and lower side (T_l) of the brazing area versus cycle number. The temperature of the upper side of interface area increased in the middle of the cyclic test but, after this, the temperature becomes stable. Marked temperature increase due to material degradation was not observed until the number of 1000 cycles. Results from the surface temperature distribution measurement showed that temperature of the local edge area of the surface rose when the temperature of the upper side of the brazing area rose. SEM observation after the heat load tests showed that there was no degradation on the surface irradiated by electron beams. It is assumed that the temperature rise of the upper side decreased due to some kind of re-bonding as the number of cycles increased. It is necessary to perform cross-sectional investigations of the brazing area of the mockup.

3.2. Comparison with calculated results for thermal response

Fig. 6 shows the experimental data with an overlay of temperature data calculated by ABAQUS. Circles and triangles show the experimental results and lines show the calculated results. Upper, middle and lower data show the results of the temperature of the surface, the

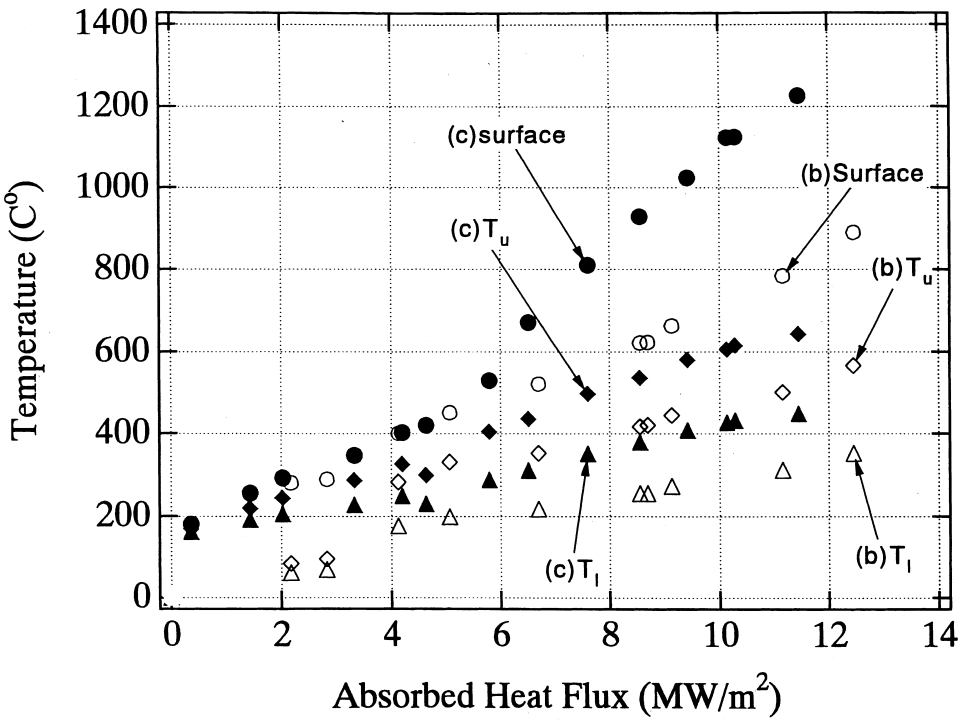

Fig. 3. Steady state temperature of MFC-1 mockup at most and least aggressive cooling conditions which correspond to (b) and (c) in Table 1. Circle (Surface), diamond (Tu) and triangle (T_l) show temperatures on surface, upper side and lower side of the brazed area.

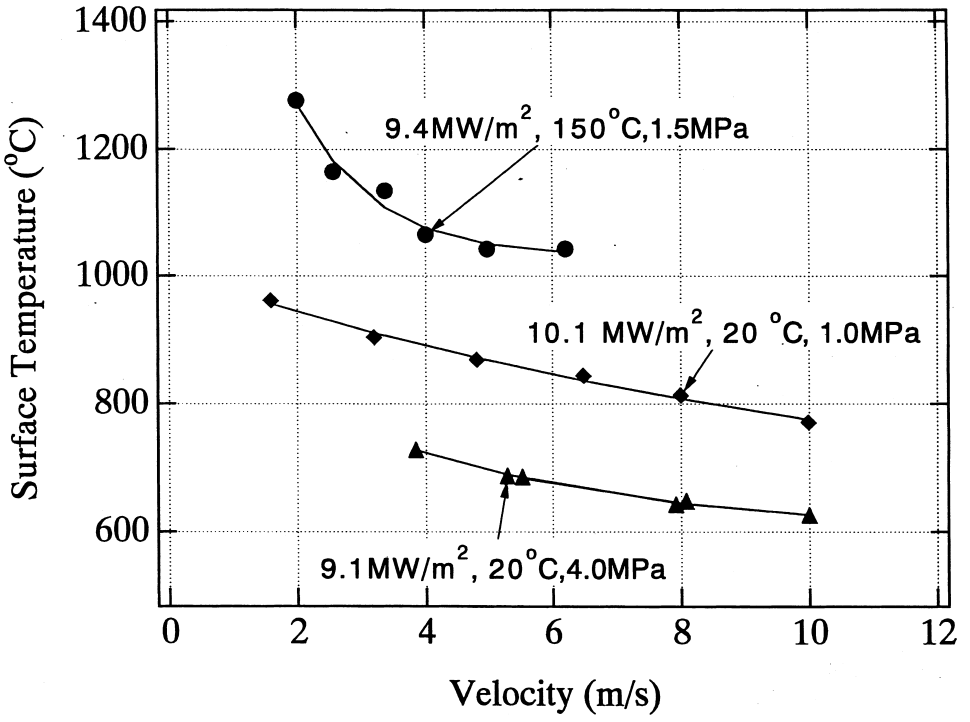

Fig. 4. Surface temperature of the MFC-1 mockup at steady state as a function of the water velocity.

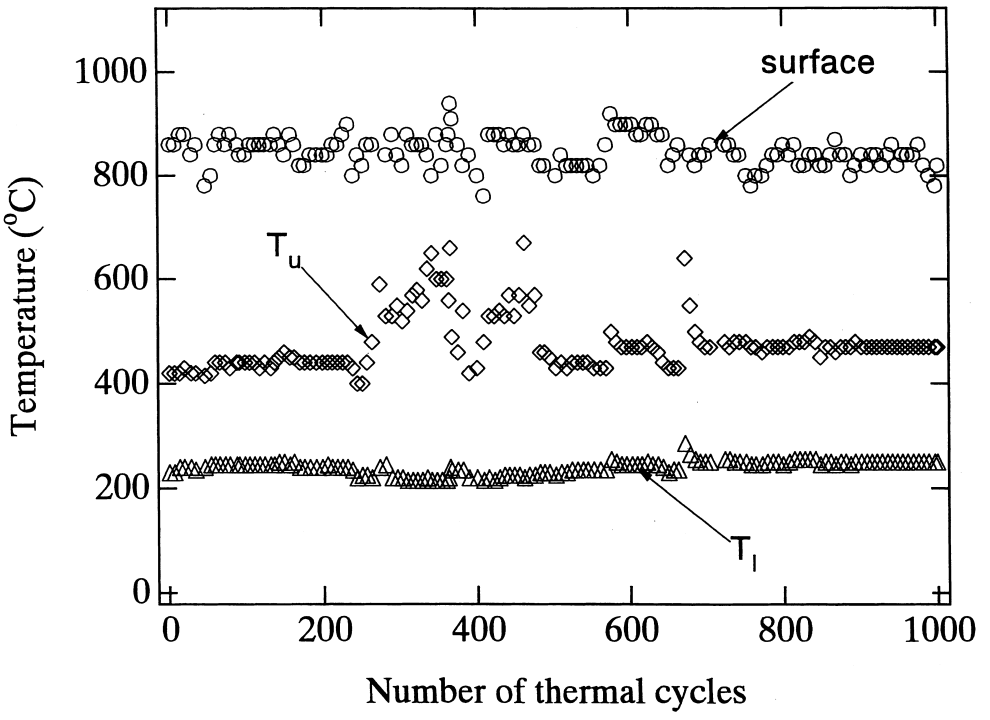

Fig. 5. Temperatures on surface, upper side and lower side of the brazed area during the thermal cycle test of MFC-1 mockup.

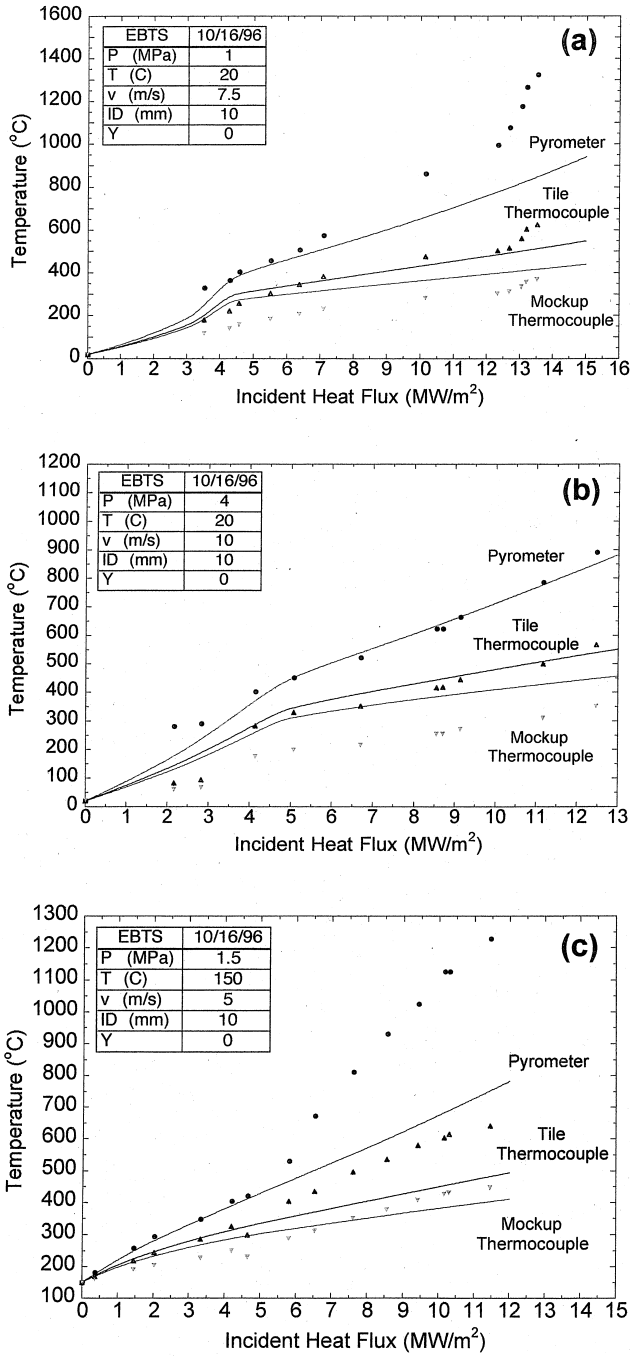

Fig. 6. Comparison of experimental with calculated data. (a) Inlet water temperature, pressure and velocity was 20°C, 1.0 MPa and 7.5 m/s, respectively. (b) Inlet water temperature, pressure and velocity was 20°C, 4.0 MPa and 10.0 m/s, respectively. (c) Inlet water temperature, pressure and velocity was 150°C, 1.5 MPa and 5.0 m/s, respectively.

upper side and lower side of the brazing area, respectively. In the case of (b), the calculated data show relatively good agreement with the experimental results for the surface temperature and the temperature of the upper side of the brazed area but, the measured temperatures of the lower side are lower than the calculated results. It is assumed that this is because heat transfer was three dimensional in the experiment but, the cal-

culation was carried out at a condition of two dimensional analysis. It is expected that this is a normal thermal response curve, indicating no damage to tile, and only pre-critical heat flux (CHF) behavior. In the case of (a), the calculated data show relatively good agreement with the experimental results for the surface temperature and the temperature of the upper side of the brazed area at low heat flux but, there is a marked difference between the calculated and experimental results at high heat flux. It is assumed that the deviation of measured temperatures from ABAQUS predicted temperature at about 12–13 MW/m^2 was most likely due to post-CHF reduction in local heat transfer film coefficient at the wall. This is clear because all three measures show the same upturn in temperature slope at 12–13 MW/m^2, indicating that local CHF has been exceeded. It is not interpreted as a detachment of the tile. In the case of (c), this shows a dramatic change in slope for the pyrometer at 6 MW/m^2. For comparison purpose, wall critical heat flux (q_w^{CHF}) was calculated using Tong-75 correlation [16]. This showed that (q_w^{CHF}) of (a)–(c) are 19.44, 28.33 and 6.06 MW/m^2, respectively. Peaking factors used were 1.8, 1.8 and 1.6, respectively. This suggested that the safety margin is necessary to be about 1.5 in the case of (a). In the case of (c), detached point of the surface temperature between the experimental and calculated results is coincident with the CHF prediction.

4. Summary

(1) Thermal response tests of the MFC-1 mockup were performed under the condition that the water flow velocity, pressure and temperature were 1.6–10 m/s, 1.0–4.0 MPa and 20°C, 150°C respectively. The MFC-1 mockup showed good heat removal performance.

(2) In the case of CX-2002U, surface temperature is nearly 1000°C at 10 MW/m^2. Therefore, use of CX-2002U, as armor material is allowable concerning temperature rise due to heat flux.

(3) Thermal fatigue test of the MFC-1 mock was also performed. Temperature increase due to degradation was not observed until the number of 1000 cycles.

(4) The comparison with measured and calculated data presented information of CHF and detachment of the tile.

Acknowledgements

One of the authors (K.T.) would like to thank Dr. I. Fujita of Hokkaido University for useful comments and discussions. Mitsubishi Heavy Industries, Ltd. is also thanked for supply of samples. The authors would like to thank Dr. M. Ulrickson of SNL for support. Finally, the author issues heartfelt thanks to Ms. P. Stevens of SNL for invaluable contributions. This work was supported in part by the Japan–USA fusion Cooperation between the Japanese Ministry for Education, Science and Culture and DOE of USA.

References

[1] O. Motojoma, N. Ohyabu, A. Komori, N. Noda, K. Yamazaki, H. Yamada, A. Sagara, S. Yamaguchi, K.Y. Watanabe, N. Inoue, H. Suzuki, Y. Kubota, J. Yamamoto, M. Fujiwara, A. Iiyoshi, Trans. Fusion Technol. 27 (1995) 123.
[2] N. Noda, Y. Kubota, A. Sagara, N. Ohyabu, K. Akaishi, H. Ji, O. Motojima, M. Hashiba, I. Fujita, T. Hino, T. Yamashina, T. Matsuda, T. Sogabe, T. Matsumoto, K. Kuroda, S. Yamazaki, H. Ise, J. Adachi, T. Suzuki, Fusion Technol. 1 (1993) 325.
[3] I. Fujita, Y. Hirohata, T. Hino, T. Yamashima, Y. Kubota, N. Noda, O. Motojima, T. Sogabe, T. Matsuda, K. Kuroda, J. Nucl. Mater. 241–243 (1997) 1185.
[4] Y. Kubota, N. Noda, A. Sagara, R. Sakamoto, O. Motojima, I. Fujita, T. Hino, T. Yamashina, K. Tokunaga, N. Yoshida, Fusion Eng. Design (to be published).
[5] A.R. Raffray, G. Federici, J. Nucl. Mater. 244 (1997) 85.
[6] G. Federici, A.R. Raffray, J. Nucl. Mater. 244 (1997) 101.
[7] K. Ioki, K. Namiki, S. Tsujimura, M. Toyoda, M. Seki, H. Takatsu, Fusion Eng. Design 15 (1991) 31.
[8] T. Matsuda, T. Sogabe, K. Kuroda, Proc. Japan-US Workshop P243 on High heat Flux Components and Plasma Surface Interaction for Next Fusion Devices, 1995, p. 366.
[9] D.L. Youchison, J.M. McDonald, L.S. Wold, in: A.M. Khounsary, T.W. Simon, R.D. Boyd, A.J. Ghajar (Eds.), Heat Transfer in High Heat Flux Systems, HTD-vol. 301, The American Society of Mechanical Engineers, 1994, p. 31.
[10] K. Kubota, N. Noda, A. Sagara, N. Inoue, K. Akaishi, O. Motojima, NIFS-MEMO-13, 1994.
[11] Hibbitt, Karlsson, Sorensen, Version 4-8 Finite Element Analysis Code, Pawtucket, RI, 1992.
[12] M. Ozisik, in: Heat Transfer – A Basic Approach McGraw-Hill, New York, 1985, p. 300.
[13] R. Thom, W. Walker, W. Fallon, G. Resing, Symposium on Boiling Heat Transfer in Steam Generating Units and Heat Exchangers, Institute of Mechanical Engineers Paper No. 6, Manchester, London, 1965.
[14] I. Fujita, private communication.
[15] Y. Kubota, N. Noda, A. Sagara, N. Inoue, K. Akaishi, Z. Yamamoto, O. Motojima, NIFS-MEMO 16, 1995.
[16] L. Tong, A phenomenological study of critical heat flux, ASME 75-HT-68, 1975.